Nonlinearity Cancellation in Fiber Optic Links Based on Frequency Referenced Carriers

N. Alic, *Member, IEEE*, E. Myslivets, E. Temprana, B. P.-P. Kuo, and S. Radic, *Member, IEEE*

***Abstract*—We study the limitations and their origins in the nonlinear effects mitigation in fiber-optic communication systems. The carrier frequencies uncertainty and their stochastic variations are identified as the major impeding factor for successful inter-channel nonlinear impairments management. Furthermore, the results clearly point out to the significant benefits of employing fully frequency referenced carriers in transmission, with frequency combs representing an immediately available solution. Finally, frequency referenced transmitters and/or receivers are shown as critical for availing longer reach at high spectral efficiencies in transmission.**

***Index Terms*—Equalization, fiber optic communications, nonlinear fiber optics.**

I. Introduction

NONLINEAR impairments represent both the main impediment to achieving the full capacity of fiber optic transmission systems [1]–[8], as well as a prime subject of scientific interest [9]. Indeed, except Raman [10], [11] and parametric amplifications [12], [13] as well as the passing interest in solitonic systems [14]–[16], nonlinear effects have always represented an obstacle to signal integrity retention in fiber optic communication [17], as well as in other areas relying on (propagation in) optical fibers for, e.g., sensing [18], and/or microwave photonics [19]. This trend has been continued even in the highly sophisticated coherent transmission systems that depend heavily on digital signal processing (DSP) [20]–[31].

The approaches to nonlinearity mitigation for transmission systems have been many—ranging from power level optimization [22] to transmission dispersion map engineering [32]–[43], to name a few. Recently, the ascendance of computational power and technological ability for real-time processing have availed a new class of mitigation approaches for nonlinear impairments in transmission: the digital back-propagation (BP) has been introduced for nonlinearity cancellation in transmission [44]–[73]. This approach aims to achieve mitigation of the nonlinear impairments by resorting to a numerical computation, in effect attempting to invert the nonlinear effects aggregated in propagation. The BP has, however, had a limited success in practice so far. In brief, the obstacle to fully equalizing nonlinear impairment is two-fold. On the one hand, the capability to mitigate the nonlinear response is bounded by the acceptable computational complexity, which still mandates rather modest amounts of mitigation in practice. More importantly, however, the mitigation has been, most often, implemented (or investigated) for per-channel basis in transmission systems [44]–[73]. Consequently, as implemented, the BP has been limited to mitigating the nonlinear effects due to single-channel propagation, encompassing self-phase modulation, which only represents a minor part of the overall nonlinear impairment [17].

Generally speaking, the described state of affairs is at the least surprising, considering that the nonlinear impairment (as far as the signal–signal interaction, rather than signal-noise mixing is concerned) is a deterministic effect, and thus, should be effectively mitigated, if not fully cancellable. Nevertheless, there has neither been a demonstration, nor a successful theoretical analysis of the limited success in effective mitigation of the nonlinear Kerr impairment in transmission to date.

Assuming a different perspective, the application of optical combs to optical communications has become of age only recently. Among the numerous implementations only the parametric combs have been demonstrated as capable of cost-effective and quality-wise satisfaction of the industry standards in transmission [74]. In effect, only the wide-band parametric combs [75]–[81] have been demonstrated as capable of flexibly covering the contiguous conventional (C-) and long (L-) transmission bands with linewidth matching those of the commercial oscillators, at a fraction of power dissipation of the latter [74].

In this contribution, we single out and demonstrate that the main limitation to nonlinearity cancellability, in effect, lays in the carrier frequency uncertainty, as well as in its stochastic variation. We furthermore show that transmission based on frequency mutually locked sources, of which the optical combs represent an immediately available implementation, allows for a complete cancellation of Kerr-based impairments in transmission, with the ultimate transmission reach being limited only by the stochastic effects.

II. Theoretical Preliminaries

The field propagation in optical fibers is governed by the nonlinear Schrödinger equation [82], taking into account only the instantaneous electronic part of the nonlinear response:

$$\frac{\partial A}{\partial z} = i\gamma |A|^2 A - \frac{\alpha}{2}A - \frac{i}{2}\beta_2 \frac{\partial^2 A}{\partial t^2} + \frac{1}{6}\beta_3 \frac{\partial^3 A}{\partial t^3} \qquad (1)$$

Manuscript received March 5, 2014; revised May 17, 2014; accepted May 23, 2014. Date of publication June 19, 2014; date of current version July 19, 2014.

N. Alic is with the Qualcomm Institute, University of California San Diego, San Diego, CA 92093-0407 USA (e-mail: nalic@ucsd.edu).

E. Myslivets, E. Temprana, B. P.-P. Kuo, and S. Radic are with the Department of Electrical and Computer Engineering, Jacobs School of Engineering, University of California San Diego, San Diego, CA 92093 USA (e-mail: ymyslive@ucsd.edu; etempran@ucsd.edu; p2kuo@ucsd.edu; sradic@ucsd.edu).

Color versions of one or more of the figures in this paper are available online at http://ieeexplore.ieee.org.

Digital Object Identifier 10.1109/JLT.2014.2332234

with *A* representing the field complex envelope, β_i's, the Taylor expansion coefficients of the mode propagation constant, capturing the dispersive waveguide properties, α, the fiber attenuation and γ the fiber nonlinear coefficient. As inferred by the most often employed numerical method for solving the propagation evolution (i.e., the split step method [82]), the terms in Eq. (1) are often separated into the nonlinear operator/effects responsible for the nonlinear interactions (i.e., the first term on the right-hand side of Eq. (1)), as well as the Linear operator, encompassing the remaining terms in Eq. (1).

In this contribution, we focus on the theoretical reversibility of nonlinear effects, and thus, consider only a single polarization case of propagation, as implied by Eq. (1), in the absence of the stochastic effect of polarization mode dispersion. In principle, the nonlinear dynamics of Eq. (1) is well behaved and integrable [83]–[85], in that it yields a stable (although perhaps difficultly obtained in a closed form [82]) solution for a given input condition [84] and at power levels of interest in transmission systems. A corollary to the previous statement is that the nonlinear effects in propagation, at least those pertinent to the Kerr response of silica fibers, were proven to be reversible [86]. In sharp contrast, however, attempts to rid the transmission of the deleterious nonlinear impairment have been limited, in simulations and in practice alike [44]–[73], [87]–[89]. The inability to equalize the nonlinear impairment has led to the definition of the power-dependent bound to the capacity in optical communications [1]–[4], [6]–[9]. The main motivation for this contribution is to investigate this apparent discrepancy with the independently established theoretical reversible property of the Kerr interactions in a deterministic, time invariant transmission channel.

The input condition to the propagation equation (1), consisting of the information streams on M wavelength division multiplexed (WDM) channels can be represented as follows:

$$A_{\mathrm{tot}}(z=0;t) = e^{-i\omega_c t}\cdot \sum_{m=1}^{M} e^{-i[(\omega_m+\delta\omega_m(t))t+\delta\phi_m(t)]}\cdot \sum_{k} A_{m\,k}\, p\,(t-kT). \tag{2}$$

In Eq. (2), ω_c denotes the central frequency of the optical field, ω_m is the expected value of the carrier frequency offset of the channel *m* (in the set of M channels considered) relative to the central frequency, and $p(t)$ is the information waveforms' generating pulse shape (assumed to be shared by all the channels in the system, which in no way limits the conclusions of the ensuing study). Furthermore, it is assumed that the pulse shape is free of intersymbol interference throughout. The $A_{m\,k}$ (in Eq. (2)) are the transmitted symbols realizations taken from a given alphabet set $\{A_m\}$. In particular, $\delta\omega$ and $\delta\varphi$ in Eq. (2) represent stochastic variations of the information carriers' (angular) frequency and phase, respectively. The finite stochastic variations of the two quantities aforementioned have always been present in optical communication systems and stem from the system design based on discrete, and independent (often referred to as free-running) laser oscillators. Two aspects of the initial condition (2) are of particular importance in our consideration. First, unlike for the linear operator (i.e., for the linear part of Eq. (1)), it is easy to demonstrate that the Fourier basis is not the proper eigenbasis for the propagation equation (1) [90]. In the last statement, the notion of eigenfunction is assumed as that input function that can pass through a (dynamical) system unperturbed, except for a possible scaling by a (complex) factor. Unlike the classical NLS equation (i.e., Eq. (1) without loss and β_3 terms), having the eigenfunctions in the form of solitons [82], [90], the presence of loss and higher order dispersion has made the pursuit of eigenfunctions of Eq. (1) futile, so far [84]. More importantly, a simple substitution of a solution in the form $A(z=0,t) = a\cdot\exp(-i\,\omega_c t)$ does not result in a common, separable $\exp(-i\,\omega_c t)$ term, typical of the eigenfunction factorization [91]. As a consequence, perturbations in frequency of the input condition (2), and in particular with respect to the nonlinear operator, can excite much more considerable perturbation of the output (i.e., the solution), after propagation through a transmission link. In simple terms, even miniscule (e.g., 0.1%) variations of the information carriers' frequency offsets with respect to the channel separation may have significant impact on the system output, due to the nonlinear interaction described by Eq. (1).

As a second important consideration with regards to the Eq. (2), it is not only that the exact positions of the laser frequencies are not known precisely, worse yet, they are in practice randomly varying. With respect to the latter observation, it is self-evident that the introduction of the time-varying initial condition (2) in conjunction with the propagation equation (1), shall jointly lead to a stochastically varying output. Furthermore, owing to the fact that carrier frequency displacement is not a perturbation of an eigen quantity, its consequence on the output variation can be of a much more considerable impact than intuitively expected. Consequently, even though the information-bearing waveforms' propagation obeys strictly deterministic laws, the uncertainty of the underlying carrier(s) (or the WDM channels) location and their phases lead to a stochastic variation of the output, rendering the nonlinear crosstalk appearing as a non-stationary stochastic effect, not amenable to successful equalization. This stochastic evolution, even in the case of strictly constant fiber properties results primarily from two effects: 1) mutual channels' walk-off, and 2) the induced variation of the input power profile. The perturbation of the walk off is a consequence of the frequency dependence of the index of refraction. As a qualitative example, note that a displacement of a carrier frequency by 160 MHz will cause an unaccounted for walk-off of the channel by half a symbol slot in a 25 GBaud system over 1000 km, and will lead to significant errors (and thus, penalties) in the cancellation of the distributed nonlinear interactions. The effect of the power profile variation caused by the carrier frequency offset is often overlooked and requires some illustrative examples. Fig. 1 shows an excerpt of the power profile variation caused by changing the carrier frequency position by a mere 50 MHz of the middle channel only, among 15 channels—with the remaining 14 channels maintaining their fixed equidistant positions. As seen in Fig. 1, even as small a deviation as 50 MHz of the carrier frequency of a single channel with respect to its assumed (i.e., ITU-grid) position, causes substantial differences in the overall field complex

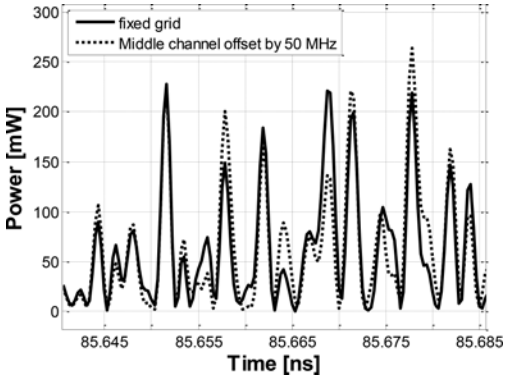

Fig. 1. The effect of a 50 MHz dispacement of the central channel in a 15-channel-count WDM system on the overall power profile at the transmiting end.

amplitude power profile. It ought to be understood that this variation of the input condition will cause a variation in the ensuing power-profile-driven nonlinear interaction in propagation (and ultimately at the output), to an extent commensurate with the level/accumulation of the nonlinear interaction. The exact quantification of this degradation will be examined in the next section. Notably, the effect of the frequency displacement (or variation) ought to be greater for systems with a higher impact of nonlinearity, thus those with higher signal powers, and/or at longer propagation distances.

In consequence to the aforementioned analysis, in the absence of stochastic effects such as the polarization mode dispersion, the Kerr effect-imposed impairments are fully reversible, on the account of the absolute knowledge of the carriers' frequencies and phases of the WDM channels. As a means of corroborating the aforementioned statement (i.e., confronted with the unattainable closed-form solution), we provide a reversal of the nonlinear propagation by back propagation—namely simulating the evolved nonlinear effects' outcome in a link with the inverse signed physical properties/constants (i.e., loss—if expressed in units of decibel per unit length, dispersion terms and fiber nonlinearity). As far as the BP, it can be performed either on the received signal (i.e., taking the form of equalization), or at the transmitter by pre-distorting the information bearing waveforms so as to attain the cancellation of the nonlinear effects at the receiver. While traditionally executed at the receiver end, BP through pre-distortion theoretically represents a better proposition: the transmitter-end implementation is devoid of amplified spontaneous emission (ASE) noise in the virtual (i.e., computational) part of the link. This property is recognized as beneficial with respect to the alternative receiver-end BP, since in the latter, the two-fold propagation of the noise-polluted signal (i.e., once in the physical link, followed by its simulated propagation in the nonlinear equalizer/solver) can lead to a deterioration in performance (e.g., by noise amplification, as in any non-unitary transfer function equalizer [92]). Additionally, in order to achieve complete reversal of the nonlinear interactions, the optical field ought to be presented to the nonlinear solver/equalizer in entirety. This has never been performed in the receiver-end BP in practice, since only part of the field corresponding to the WDM channels is ever detected at the receiver end. Consequently, the four-photon mixing products that had leaked out of the transmitted band are omitted in traditional BP mitigation, thereby preventing a full realization of the impairment reversal. For the considerations of noise corruption and field representation, all simulations in this study were performed assuming pre-compensation, with a generalized block diagram shown in Fig. 2. In essence, the "pre-distortion" block acquires the information frames to be imprinted onto the WDM channels and pre-computes the joint BP pattern that is subsequently distributed and modulated onto optical carriers. Concentrating on the simulations for the moment, it is well known that the accuracy of a symmetric split step [82] simulation is proportional to the cube of the step size. Therefore, ability of reaching the reversal of the nonlinear interactions may demand vanishingly small step-size even in the absence of noise, since the accumulation of stochastic numerical errors prevents the full reversibility akin to the noise accumulation in propagation. The requirement for a high numerical accuracy was corroborated in an accurate split-step method-based long-haul propagation simulation of 15 WDM channels on a strictly fixed frequency grid. The simulation (parameters shown in Table I, with the exception of amplifier noise figure) was implemented as a symmetric split step with a maximal allowed phase change per step of 5×10^{-4} degrees in a developed graphic-processing-unit (GPU)-assisted solver. The results of the noiseless simulation are shown in Fig. 3.

As seen in Fig. 3, the transmission (in the absence of noise) of up to 10 000 km yielded no variation in performance, thus indeed demonstrating a full reversal of nonlinear effects. Although all the simulations in this paper have been performed for QAM modulation format, the approach is of general applicability and can be employed with arbitrary signals, including orthogonal frequency division multiplex (OFDM), or even analog signals. Considering the associated computational complexity, the results shown in Fig. 3 have little practical value at this moment. Nevertheless, they do establish the possibility of full cancellation of the deterministic (i.e., signal–signal) interactions in propagation. All results presented in this paper were quantified by the worst case Q factor estimated as the minimal Euclidean distance between the nearest constellation points' separation, divided by the corresponding variance [92]. The observed enhanced performance of the channels toward the edges in Fig. 3 is a consequence of the pulse shape used in the simulations. Specifically, each of the WDM channels in this simulation were shaped by a regular fourth-order Bessel filter, resulting in a finite spectral overlap between the neighboring channels (i.e., a finite linear crosstalk) and the observed 3 dB superior performance of the channels 1 and 15 is a consequence of those channels having only a single (linearly) interfering neighbor, rather than two interferers, pertinent to the rest of the "inner" channels in the system. In contrast to the results shown in Fig. 3, corresponding to the perfect knowledge of the channels carrier frequencies, in the next section, we quantify the penalty associated by the relative frequency offsets of the information carriers, commonly present in the existing systems.

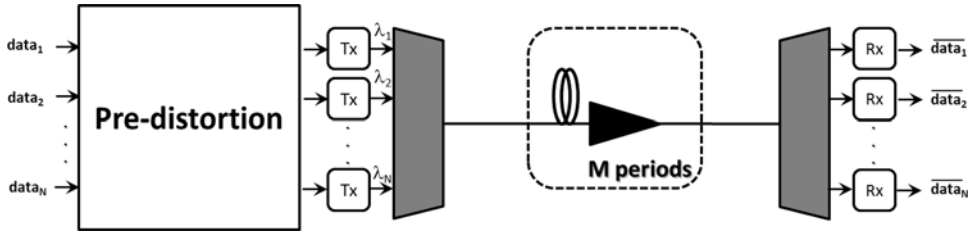

Fig. 2. A nonlinearity cancellating system schematic: The information-bearing waveforms imprinted onto the WDM channels are pre-computed in a pre-distortion profile calculator, taking into account the information to be transmitted on all channels simultaneously, as well as the physical system characteristics. The pre-distortion calculation is performed for a link having the inverse signed physical characteristics, as well as the mirror image of the propagation power profile of the physical link.

TABLE I
SIMULATION PARAMETERS

Parameter	Value
Dispersion	16 ps/nm·km
Dispersion Slope (S)	0.06 ps/nm^2·km
Nonlinear Index (n_2)	2.6×10^{-20}m^2/W
Effective are A_{eff}	80 μm^2
Loss (α)	0.2 dB/km
Amplifier span	100 km
Amplifier noise figure	4 dB

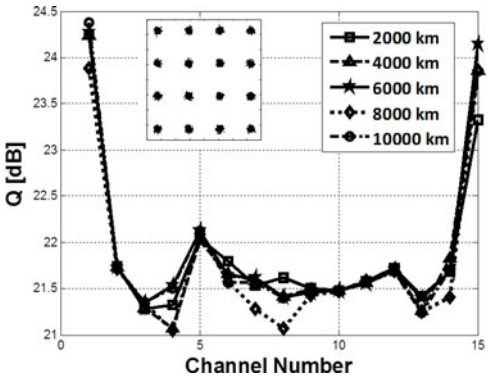

Fig. 3. Full reversibility of 15-channel 25 GBaud 16 QAM propagation with a 2 dBm lauch power per channel per span for distances up to 10 000 km with 100 km amplifier spans in a noiseless simulation of a fully frequency fixed grid.

III. THE EFFECT OF THE CARRIER FREQUENCY DISPLACEMENT

This section investigates the effect of carrier frequency wander and its implication on the nonlinear impairments' mitigation. The implemented simulation engine consisted of two parts, the pre-distortion calculator (i.e., the virtual link), and a physical link simulator. In the first engine, the randomly seeded PRBS data (with different initial condition per channel) were first mapped to 16 QAM symbols with Gray mapping, and subsequently, imprinted onto the corresponding carriers (i.e., laser oscillators) by means of band limited Mach–Zehnder (MZI) modulators, including pre-distortion of the waveforms ensuring the optimized constellation generation. The propagation was simulated in a NLS solver (with a symmetric power evolution to that of the physical link and with the opposite sign physical constants to that of the physical link). The output electric field of the pre-distortion engine was first wavelength demultiplexed, and then, homodyne received The thus-obtained analog I and Q electrical components for each channel were conveyed to a set of transmitters (of the physical link) in each of which the electrical signals are pre-distorted in order to achieve the 1-to-1 mapping of the received fields (in the virtual link) and those that would be propagated in the physical link. The pre-distorted I and Q components are imprinted to the physical link carriers having a 10 kHz linewidth by means of fourth order Bessel function 25 GHz MZI's. Upon propagation through the physical link part (modeled by the standard NLS solver), the channels are de-multiplexed, coherently detected (in a bank of band-limited coherent receivers) by randomly seeded 10 kHz local oscillators, and after the standard train of DSP procedures (carrier phase recovery, timing recovery—note that the dispersion is already compensated for by means of pre-distortion), the constellations were extracted for performance estimation.

Fig. 4 shows the Q factor estimated over 2^{12} symbols in a 15-count 50 GHz-spaced WDM system carrying 25-GBaud 16 QAM data shaped by raised cosine filters [92] with a 10% roll-off factor. The channels were set to propagate at various powers per channel at launch (i.e., 0, 3, and 6 dBm) over a distance of 1000 km, consisting of 10 spans of standard single mode fibers with inline erbium-doped fiber amplifiers characterized by a noise figure of 4 dB fully compensating the fiber loss in each span. In order to determine the efficacy of the nonlinear effect compensation, all the simulations, henceforth, have been performed with an allowed phase change of 0.01 degrees per nonlinear step. For a reference, in Table II shown are the results of an uncompensated system, system with "per-channel BP," as well as the joint multi-channel BP in the case of frequency-referenced carriers. The last column in Table II is demonstrative of a significant performance improvement provided by the joint multichannel BP.

For the sake of maintaining tractability of the system behavior, only the carrier frequency of the central channel was displaced by a shift ranging from 50 to 500 MHz (i.e., from 0.1% to 1% of the standard ITU standard grid separation). Meanwhile, the pre-distortion calculation was performed for a perfectly equidistant grid, as is done in standard practice. As implied by the results shown in Fig. 4, a displacement of as little as 50 MHz yields a prominent penalty for high average powers (i.e., 6 dBm)—a 2-dB Q-degradation is observed and is clearly related to the diminished ability of reversing the nonlinear effects. With a further

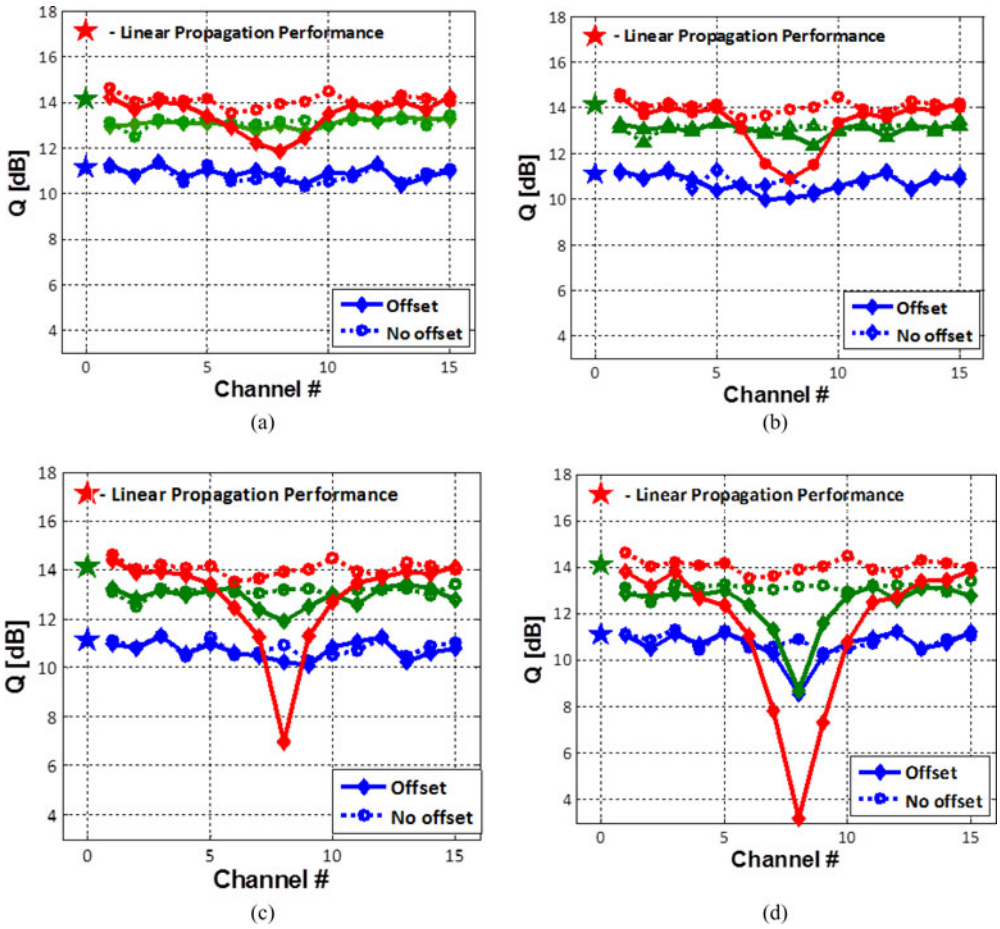

Fig. 4. The effect of the middle channel (only) frequency displacement in a 15-count WDM system with 100 km amplifier spans (with a fixed 4 dB noise figure amplifiers) at the 1000 km propagation distance. In each figure part, the performance for three different lauch powers per channel per span are shown: 0 dBm in blue, 3 dBm in green, and 6 dBm in red. For each of the powers, dashed line shows performance on an unperturbed – stricly periodic 50 GHz frequency grid, with solid lines showing the performance affected by the frequency offset. Stars at the 0 Channel number abscissa denote the ideal linear propagation performance–in the absence of nonlinear effects, for each of the average launch powers per span considered.

TABLE II
A15 CHANNEL 1000 KM 16 QAM PERFORMANCE OVERVIEW FOR THE CASES: (I) NO NONLINEARITY CANCELLATION; (II) PER-CHANNEL BP; (III) JOINT MULTI-CHANNEL BP

Power [dBm]	No compensation Q [dB]	Per Channel BP Q [dB]	Multi-channel BP Q [dB]
0	4.9	8.2	11
3	n/a	4.2	13
6	n/a	n/a	14

offset increase, a 100 MHz frequency displacement induces an additional 1-dB penalty for 6 dBm launch power, while having virtually no effect on the two lower launch powers per channel considered. Yet a further increase in the carrier frequency deviation incurs observable penalties even for low launch powers. In particular, while the 200 MHz offset incurs a significant 7 dB penalty (for the central channel) at a high 6 dBm power, even a moderate power level (3 dBm) exhibits an obvious departure from the ideal performance. More prominently, the carrier frequency excursion by 500 MHz (i.e. 1% of the ITU channel spacing) causes a complete dissipation of information and irreversible penalties for the high (6 dBm) power levels. Meanwhile, 4.5 and 2 dB penalties are incurred for the launch powers of 3 and 0 dBm per span for the latter frequency displacement, respectively. The result shown in Fig. 4 bears another important characteristic. The nonlinear impairment in fiber optic transmission bears a notion of mixing [17], [82], [86] (as a consequence of the $\chi^{(3)}$ nature of the silica response). Qualitatively speaking, the propagating WDM channels walk off through one another (at a rate defined by their frequency separation and the group velocity dispersion of the fiber), which induce a mutual phase modulation and mix their pertinent information content. The nonlinear equalization by means of the underlying interaction reversal attempts to inverse this power flow. However, the displacement of the (central) channel(s) from its assumed location perturbs the launch waveform and its subsequent evolution due to the associated deviation of the channel's walk-off rate, thus resulting in an incomplete reversal of the mixing products to their original source(s) (i.e., channel(s)). As seen in parts of Fig. 4(a)–(c), this information transfer for moderate power

levels and frequency displacements is contained to the nearest neighbors. Indeed, not only does the physically displaced channel suffer from a performance degradation, but the perturbation of the field evolution causes incomplete nonlinear crosstalk reversal. The latter leaves a part of the distortion residual in the neighbors, and in turn, affects their performance.

With a further displacement increase, the described trend is only exacerbated, ultimately leading to a complete loss of information in the central (i.e., displaced) channel. As implied by the results in Fig. 4(d), the described catastrophic path significantly affects the nearest neighbors and proliferates to the further surrounding channels. Overall, the observed catastrophic loss of information in the central channel [see Fig. 4(d)] affects the performance of as many as six surrounding channels (i.e., three on each side of the central channel). From a different perspective, the results shown in Fig. 4 attest to the locality of the nonlinear interaction. In effect, for the SMF physical properties (most notably its dispersion), the nonlinear interaction is contained to seven nearest neighbors, with a major part of the interaction being contained to a total of five nearest neighbors.

In Fig. 4, also shown is the performance of the ideal linear propagation (i.e., in the absence of nonlinear effects), denoted by stars at the zeroth channel abscissa. As can be seen, unlike the noiseless propagation shown in Fig. 3 where full reversal of nonlinear interactions is achieved, results in Fig. 4 clearly exhibit a residual penalty in the presence of noise, which grows with the average launch power per span. The observed residual penalty is a consequence of the nonlinear phase noise [54], [93], which represents the ultimate bound on the achievable performance, as well as the capacity. Furthermore, due to the walk-off proportionality to the product of the frequency displacement and the propagation length, penalties comparable to those shown in Fig. 4 shall be incurred for even smaller frequency offsets, at longer propagation distances, inversely proportional to the frequency offset.

On the other hand, in the absence of nonlinearity (i.e., strictly linear systems, similarly to the radio communications, or a low-power operated fiber optic transmission link), the carrier and phase wander correspond to the perturbations of the underlying harmonic eigenfunctions that, at the output, are manifested as simple time shifts, or rotations of the electro-magnetic field. The system dynamics of this kind resembles plain unitary transformations, thus lending themselves to simple (lumped) corrections that are trivially realized through DSP in practice. In sharp contrast, longitudinally distributed and power-dependent nature of Kerr interaction implies that the absence of the absolute frequency reference will yield intractable (irreversible) mixing products at the transmission system receiving end. Fig. 4 also points to the fundamental inability of the BP to tackle multichannel nonlinear cross talk in transmission systems without an accurate knowledge of the absolute position and the relative separation of the channels' carrier frequencies, let alone their stochastic wander. It is also important to emphasize that in practice, currently employed lasers can easily wander by as much as several gigahertz from their nominal position [94], with an average near-term stability of 300 MHz [95], making the findings of this study all the more relevant to the practical systems.

Opposed to the scenario considered in the preceding set of simulations, we consider propagation based on frequency-referenced carriers. These carriers can, for instance, be realized by frequency combs serving as a bank of information carriers. While frequency combs are not free from frequency fluctuations in general, owing to the fact that these coherent multi-wavelength emitters are driven by a single master oscillator [75], [77], [79], all of the constituent lines in the comb cascade experience highly correlated, joint frequency offsets [75]. The latter form of joint channel displacement in no way alters the launch power profile (consider Eq. (2) and Fig. 1), thus leaving the displacement-caused walk-off perturbation the only remnant cause of incomplete restoration of the nonlinear interaction. Indeed, the joint displacement of the channels maintains the walk-off rate, to the extent allowable by the magnitude of the second-order (β_2) and higher order dispersion terms [82].

The results of the effect of this joint frequency wander are shown in Fig. 5. Unlike the scenario pursued in generating the result in Fig. 4, where only the central channel position was shifted, in this set of simulations, all channels were displaced by an equal frequency shift varying from -10 to 10 GHz with respective to their nominal ITU positions. Comparing the results in Fig. 5 to those from Fig. 4, the allowed carrier frequency uncertainty is increased by more than an order of magnitude for a fiber with a finite dispersion (and dispersion slope)—a carrier frequency deviation by as much as 5 GHz (i.e., 10% of the ITU grid) at the distance of 2000 km still allows a complete reversibility of the nonlinear impairment with practically vanishingly small penalty, as compared to the fully linear case of propagation. We do note that the power levels considered in the simulations may appear too high from the perspective of the existing systems. However, the elevation of the launch power is absolutely necessary for increasing both the reach and the capacity (in the information-theoretic sense [9], [96]) in the transmission systems. The joint channel BP approach, as implemented in this study, clearly enables both of those objectives. Thus, from a perspective of utilizing frequency-referenced sources in transmission, the benefits from employing frequency combs is two-fold: First, they provide the all-important referenced frequency grid for transmission systems, which the presented results have established as the pivotal factor for the successful nonlinearity mitigation. Second, in the case of the frequency wander—to which even the combs are susceptible, these frequency-referenced carriers ensure a synchronous joint displacement of the carriers, thus significantly mollifying the effect of carrier frequencies separation variation (i.e., breathing). Note that comb sources other than parametrically generated can be used for the purpose of frequency referenced carriers (i.e., mode-locked lasers, modulator combs), however, due to the associated inherent short-comings, none of the alternative sources is capable of providing both a wide spectral coverage (corresponding to at least the whole C-band), high OSNR/high power per line, as equalized a spectral response over the emission spectrum, as well as the flexible ITU-compliant frequency pitch, as those demonstrated by the parametric combs [75]–[81]. Finally, it must be equally emphasized that the comb sources' master oscillators are more than an order of magnitude more

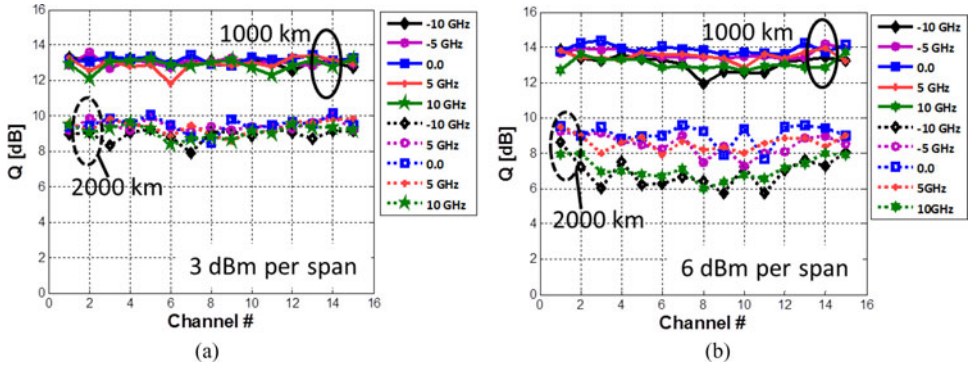

Fig. 5. The effect of a synchronous frequency offset. Performance with nonlinearity cancellation for fully frequency referenced systems with a given identical frequency offset from the assumed frequency positions in back propagation with solid lines showing performance at 1000 km and dotted lines at 2000 km for (a) 3 dBm average launch power per span, and (b) 6 dBm average power per span.

stable than the common commercial wavelength sources [74]. Consequently, comb sources provide better than 20 MHz-stable frequency grid [80], which further reinforces the employment of these emitters as the optimal solution for information carriers in high capacity transmission systems capable of reaching otherwise unattainable information capacities in transmission.

As a concluding remark to this section, we note that the results presented attest to a theoretical ability of the full reversal of signal–signal nonlinear interactions in a deterministic and stationary transmission fiber optic transmission system. Based on the findings, one can conclude that the reach and capacities in transmission are determined only by the loss [97], noise accumulation, and the associated nonlinear phase noise [93] development. Additionally, the ultimate propagation limits are set by the stochastic polarization mode dispersion and the polarization dependent loss in transmission, the effect of which will be presented elsewhere. Finally, we have opted not to present results on the effect of phase decorrelation among carriers on nonlinearity compensation in this contribution. On the one hand, the effect of the phase wander on the nonlinear compensation is much smaller with respect to that of the frequency displacement. More importantly, the phase wander is a stochastic effect with a significantly broader scope and diversity of realizations that requires a focused in-depth study and is, thus, best left for a dedicated contribution.

IV. Conclusion

We have established the carriers' frequency uncertainty and their stochastic wander as the fundamental culprits for the irreversibility of nonlinear effects in propagation in fiber optic communication systems. In particular, the presented results clearly demonstrate that even minor departures of the information carriers from their nominal location on the frequency grid render the reversal of the nonlinear interaction impossible, with departures of 500 MHz affecting even the launch power levels of 0 dBm at propagation distances of only 1000 km. The aforementioned results strongly imply benefits of frequency-referenced systems, prominently relying on optical frequency combs, as a practical means to breaking through the currently established nonlinear bounds of capacity in transmission. While the presented results have been obtained in idealized conditions, they nevertheless bear significant implications and provide substantial margins for practical implementation, and thus, pave a way to systems with extended reach and/or with high spectral efficiencies greatly unimpeded by nonlinear effects in propagation.

References

[1] P. P. Mitra and J. B. Stark, "Nonlinear limits to the information capacity of optical fibre communications," *Nature*, vol. 411, pp. 1027–1030, 2001.
[2] J. Tang, "The shannon channel capacity of dispersion-free nonlinear optical fiber transmission," *J. Lightw. Technol.*, vol. 19, no. 8, pp. 1104–1109, Aug. 2001.
[3] K. S. Turitsyn, S. A. Derevyanko, I. V. Yurkevich, and S. K. Turitsyn, "Information capacity of optical fiber channels with zero average dispersion," *Phys. Rev. Lett.*, vol. 91, no. 20, p. 203901, 2003.
[4] I. Djordjevic, B. Vasic, M. Ivkovic, and I. Gabitov, "Achievable information rates for high-speed long-haul optical transmission," *J. Lightw. Technol.*, vol. 23, no. 11, pp. 3755–3763, Nov. 2005.
[5] M. H. Taghavi, G. C. Papen, and P. H. Siegel, "On the multiuser capacity of WDM in a nonlinear optical fiber: Coherent communication," *IEEE Trans. Inf. Theory*, vol. 52, no. 11, pp. 5008–5022, Nov. 2006.
[6] R.-J. Essiambre, G. J. Foschini, G. Kramer, and P. J. Winzer, "Capacity limits of information transport in fiber-optic networks," *Phys. Rev. Lett.*, vol. 101, p. 163901, 2008.
[7] R.-J. Essiambre, G. Kramer, P. J. Winzer, G. J. Foschini, and B. Goebel, "Capacity limits of optical fiber networks," *J. Lightw. Technol.*, vol. 28, no. 4, pp. 662–701, Feb. 2010.
[8] A. D. Ellis, J. Zhao, and D. Cotter, "Approaching the non-linear Shannon limit," *J. Lightw. Technol.*, vol. 28, no. 4, pp. 423–433, Feb. 2010.
[9] E. Agrell and M. Karlsson, "Satellite constellations: Towards the nonlinear channel capacity," presented at the IEEE Photonics Conf., Burlingame, CA, USA, 2012, Paper TuM1.
[10] S. Namiki and Y. Emori, "Ultrabroad-band Raman amplifiers pumped and gain-equalized by wavelengthdivision-multiplexed high-power laser diodes," *IEEE J. Sel. Topics Quantum Electron.*, vol. 7, pp. 3–16, 2001.
[11] S. Radic, "Forward, bi-directional and higher order Raman amplifiers," in *Raman Amplifiers for Telecommunications 1*, vol. 90/1, M. Islam, Ed. New York, NY, USA: Springer, 2004.
[12] C. J. McKinstrie, S. Radic, and A. R. Chraplyvy, "Parametric amplifiers driven by two pump waves," *IEEE Sel. Topics Quantum Electron.*, vol. 8, no. 3, pp. 538–547, May/Jun. 2002.
[13] M. Marhic, *Fiber Optical Parametric Amplifiers, Oscillators and Related Devices*. Cambridge, U.K.: Cambridge Univ. Press, 2008.
[14] L. F. Mollenauer and K. Smith, "Demonstration of soliton transmission over more than 4000 km in fiber with loss periodically compensated by Raman gain," *Opt. Lett.*, vol. 13, pp. 675–677, 1988.
[15] G. M. Carter, R. Mu, V. Grigoryan, P. Sinha, C. R. Menyuk, T. F. Carruthers, M. L. Dennis, and I. N. Duling III, "20 Gb/s transmission of dispersion-managed solitons over 20,000 km," presented at the Optical Fiber Communication Conf., San Diego, CA, USA, 1999, Paper WC1.

[16] L. F. Mollenauer, P. V. Mamyshev, J. Gripp, M. J. Neubelt, N. Mamysheva, L. Grüner-Nielsen, and T. Veng, "Demonstration of massive wavelength-division multiplexing over transoceanic distances by use of dispersion-managed solitons," *Opt. Lett.*, vol. 25, pp. 704–706, 2000.

[17] A. R. Chraplyvy, "Limitations on lightwave communications imposed by optical-fiber nonlinearities," *J. Lightw. Technol.*, vol. 8, no. 10, pp. 1548–1557, Oct. 1990.

[18] R. A. Bergh, B. Culshaw, C. C. Cutler, H. C. Lefevre, and H. J. Shaw, "Source statistics and the Kerr effect in fiber-optic gyroscopes," *Opt. Lett.*, vol. 7, pp. 563–565, 1982.

[19] A. J. Seeds, "Microwave photonics," *IEEE Trans. Microw. Theory Tech.*, vol. 50, no. 3, pp. 877–887, Mar. 2002.

[20] M. G. Taylor, "Coherent detection method using DSP for demodulation of signal and subsequent equalization of propagation impairments," *IEEE Photon. Technol. Lett.*, vol. 16, no. 2, pp. 674–676, Feb. 2004.

[21] D. McGhan, M. O'Sullivan, C. Bontu, and K. Roberts, "Electronic dispersion compensation," presented at the Optical Fiber Communication Conf., Anaheim, CA, USA, 2006, Paper OWK1.

[22] S. J. Savory, G. Gavioli, R. I. Killey, and P. Bayvel, "Electronic compensation of chromatic dispersion using a digital coherent receiver," *Opt. Exp.*, vol. 15, pp. 2120–2126, 2007.

[23] E. Ip and J. M. Kahn, "Digital equalization of chromatic dispersion and polarization mode dispersion," *J. Lightw. Technol.*, vol. 25, no. 8, pp. 2033–2043, Aug. 2007.

[24] S. L. Jansen, I. Morita, T. C. Schenk, and H. Tanaka, "Long-haul transmission of 16 $\times$ 52.5 Gbits/s polarization-division-multiplexed OFDM enabled by MIMO processing (Invited)," *J. Opt. Netw.*, vol. 7, pp. 173–182, 2008.

[25] B. J. C. Schmidt, A. J. Lowery, and J. Armstrong, "Experimental demonstrations of electronic dispersion compensation for long-haul transmission using direct-detection optical OFDM," *J. Lightw. Technol.*, vol. 26, no. 1, pp. 196–203, Jan. 2008.

[26] C. R. S. Fludger, T. Duthel, D. van den Borne, C. Schulien, E.-D. Schmidt, T. Wuth, J. Geyer, E. De Man, G.-D. Khoe, and H. de Waardt, "Coherent equalization and POLMUX-RZ-DQPSK for robust 100-GE transmission," *J. Lightw. Technol.*, vol. 26, no. 1, pp. 64–72, Jan. 2008.

[27] K. Roberts, M. O'Sullivan, K.-T. Wu, H. Sun, A. Awadalla, D. J. Krause, and C. Laperle, "Performance of dual-polarization QPSK for optical transport systems," *J. Lightw. Technol.*, vol. 27, no. 16, pp. 3546–3559, Aug. 2009.

[28] M. Kuschnerov, F. N. Hauske, K. Piyawanno, B. Spinnler, M. S. Alfiad, A. Napoli, and B. Lankl, "DSP for coherent single-carrier receivers," *J. Lightw. Technol.*, vol. 27, no. 16, pp. 3614–3622, Aug. 2009.

[29] A. H. Gnauck, P. J. Winzer, S. Chandrasekhar, X. Liu, B. Zhu, and D. W. Pecham, "Spectrally efficient long-haul WDM transmission using 224-Gb/s polarization-multiplexed 16-QAM," *J. Lightw. Technol.*, vol. 29, no. 4, pp. 373–377, Feb. 2011.

[30] X. Liu, S. Chandrasekhar, B. Zhu, P. J. Winzer, A. H. Gnauck, and D. W. Peckham, "448-Gb/s reduced-guard-interval CO-OFDM transmission over 2000 km of ultra-large-area fiber and five 80-GHz-grid ROADMs," *J. Lightw. Technol.*, vol. 29, no. 4, pp. 483–490, Feb. 2011.

[31] S. Chandrasekhar and X. Liu, "OFDM based superchannel transmission technology," *J. Lightw. Technol.*, vol. 30, no. 24, pp. 3816–3823, Dec. 2012.

[32] B. Marks, W. L. Kath, and S. K. Turitsyn, "Dispersion maps with optimized amplifier placement for wavelength-division-multiplexing," presented at the Optical Fiber Communication Conf., Baltimore, MD, USA, 2000, Paper WA7.

[33] G. Mohs, W. T. Anderson, and E. A. Golovchenko, "A new dispersion map for undersea optical communication systems," presented at the Optical Fiber Communication Conf., Anaheim, CA, USA, 2007, Paper JThA41.

[34] R. Bhamber, C. French, S. K. Turitsyn, V. Mezentsev, W. Forysiak, and J. H. B. Nijhof, "Lumped dispersion mapping and performance margins in existing SMF-DCF terrestrial links," *J. Opt. Netw.*, vol. 7, pp. 106–110, 2008.

[35] L. B. Du and A. J. Lowery, "Fiber nonlinearity compensation for CO-OFDM systems with periodic dispersion maps," presented at the Optical Fiber Communication Conf., San Diego, CA, USA, 2009, Paper OTuO1.

[36] P. Harper, S. B. Alleston, W. Forysiak, and N. J. Doran, "10 Gbit/s dispersion-managed soliton transmission over 13,400 km in a weak, symmetric non-zero dispersion shifted fiber dispersion map," presented at the Conf. on Laser Electro-Optics, San Francisco, CA, USA, 2001, Paper CTuM5.

[37] D. G. Foursa, Y. Cai, C. R. Davidson, A. Lucero, M. Mazurczyk, W. Patterson, O. Sinkin, W. Anderson, J.-X. Cai, G. Redington, M. Nissov, A. Pilipetskii, and N. S. Bergano, "Long-haul coherent QPSK transmission of 40 G channels with 120% spectral efficiency using increased linearity dispersion map with 100 km spans and EDFAs," presented at the Optical Fiber Communication Conf., San Diego, CA, USA, 2010, Paper OTuD2.

[38] X. Li, F. Zhang, Z. Chen, and A. Xu, "Suppression of XPM and XPM-induced nonlinear phase noise for RZ-DPSK signals in 40 Gbit/s WDM transmission systems with optimum dispersion mapping," *Opt. Exp.*, vol. 15, pp. 18247–18252, 2007.

[39] Y. Frignac, J. Antona, and S. Bigo, "Enhanced analytical engineering rule for fast optimization of dispersion maps in 40 Gbit/s-based transmission systems," presented at the Optical Fiber Communication Conf., Los Angeles, CA, USA, 2004, Paper TuN3.

[40] F. Zhang, C. A. Bunge, K. Petermann, and A. Richter, "Optimum dispersion mapping of single-channel 40 Gbit/s return-to-zero differential phase-shift keying transmission systems," *Opt. Exp.*, vol. 14, pp. 6613–6618, 2006.

[41] C. Fürst, C. Scheerer, G. Mohs, J.-P. Elbers, and C. Glingener, "Influence of the dispersion map on limitations due to cross-phase modulation in WDM multispan transmission systems," presented at the Optical Fiber Communication Conf., Anaheim, CA, USA, 2001, Paper MF4.

[42] B. Zhu, L. Leng, L. E. Nelson, S. Stulz, T. N. Nielsen, and D. A. Fishman, "Experimental investigation of dispersion maps for 40 $\times$ 10 Gb/s transmission over 1600 km of fiber with 100-km spans employing distributed Raman amplification," presented at the Optical Fiber Communication Conf., Anaheim, CA, USA, 2001, Paper TuN3.

[43] R.-J. Essiambre, G. Raybon, and B. Mikkelsen, "Pseudo linear transmission of high-speed TDM signals," in *Fibero Optic Telecommunication IVB*, I. Kaminow, T. Li, Eds. San Diego, CA, USA: Academic Press, 2002.

[44] E. Ip and J. M. Kahn, "Compensation of dispersion and nonlinear impairments using digital backpropagation," *J. Lightw. Technol.*, vol. 26, no. 20, pp. 3416–3425, Oct. 2008.

[45] E. Mateo, L. Zhu, and G. Li, "Impact of XPM and FWM on the digital implementation of impairment compensation for WDM transmission using backward propagation," *Opt. Exp.*, vol. 16, no. 20, pp. 16124–16137, 2008.

[46] E. Yamazaki, F. Inuzuka, K. Yonenaga, A. Takada, and M. Koga, "Compensation of interchannel crosstalk induced by optical fiber nonlinearity in carrier phase-locked WDM system," *IEEE Photon. Technol. Lett.*, vol. 19, no. 1, pp. 9–11, Jan. 2007.

[47] S. Oda, T. Tanimura, T. Hoshida, C. Ohshima, H. Nakashima, Z. Tao, and J. C. Rasmussen, "112 Gb/s DP-QPSK transmission using a novel nonlinear compensator in digital coherent receiver," presented at the Optical Fiber Communication Conf., San Diego, CA, USA, 2009, Paper OThR6.

[48] L. Li, Z. Tao, L. Liu, W. Yan, S. Oda, T. Hoshida, and J. C. Rasmussen, "Nonlinear polarization crosstalk canceller for dual-polarization digital coherent receivers," presented at the Optical Fiber Communication Conf., San Diego, CA, USA, 2010, Paper OWE3.

[49] T. Tanimura, T. Hoshida, T. Tanaka, L. Li, S. Oda, H. Nakashima, Z. Tao, and J. C. Rasmussen, "Semi-blind nonlinear equalization in coherent multi-span transmission system with inhomogeneous span parameters," presented at the Optical Fiber Communication Conf., San Diego, CA, USA, 2010, Paper OMR6.

[50] L. B. Du and A. J. Lowery, "Experimental demonstration of XPM compensation for CO-OFDM systems with periodic dispersion maps," presented at the Optical Fiber Communication Conf., Los Angeles, CA, USA, 2011, Paper no. OWW2.

[51] D. Rafique and A. D. Ellis, "Various nonlinearity mitigation techniques employing optical and electronic approaches," *IEEE Photon. Technol. Lett.*, vol. 23, no. 23, pp. 1838–1840, Dec. 2011.

[52] D. Rafique, M. Mussolin, J. Mårtensson, M. Forzati, J. K. Fischer, L. Molle, M. Nölle, C. Schubert, and A. D. Ellis, "Polarization multiplexed 16 QAM transmission employing modified digital back-propagation," *Opt. Exp.*, vol. 19, pp. B805–B810, 2011.

[53] D. Rafique and A.D. Ellis, "Impact of signal-ASE four-wave mixing on the effectiveness of digital back-propagation in 112 Gb/s PM-QPSK systems," *Opt. Exp.*, vol. 19, pp. 3449–3454, 2011.

[54] D. Rafique, J. Zhao, and A. D. Ellis, "Digital back-propagation for spectrally efficient WDM 112 Gbit/s PM m-ary QAM transmission," *Opt. Exp.*, vol. 19, pp. 5219–5224, 2011.

[55] D. Rafique and A. D. Ellis, "Nonlinearity compensation in multi-rate 28 Gbaud WDM systems employing optical and digital techniques under diverse link configurations," *Opt. Exp.*, vol. 19, pp. 16919–16926, 2011.

[56] L. Zhu and G. Li, "Nonlinearity compensation using dispersion-folded digital backward propagation," *Opt. Exp.*, vol. 20, no. 13, pp. 14362–14370, 2012.
[57] L. Zhu and G. Li, "Folded digital backward propagation for dispersion-managed fiber-optic transmission," *Opt. Exp.*, vol. 19, pp. 5953–5959, 2011.
[58] E. F. Mateo, X. Zhou, and G. Li, "Improved digital backward propagation for the compensation of inter-channel nonlinear effects in polarization-multiplexed WDM systems," *Opt. Exp.*, vol. 19, pp. 570–583, 2011.
[59] L. Zhu and G. Li, "Nonlinearity compensation using dispersion-folded digital backward propagation," *Opt. Exp.*, vol. 20, pp. 14362–14370, 2012.
[60] E. F. Mateo, F. Yaman, and G. Li, "Efficient compensation of inter-channel nonlinear effects via digital backward propagation in WDM optical transmission," *Opt. Exp.*, vol. 18, pp. 15144–15154, 2010.
[61] W. Yan, Z. Tao, L. Dou, L. Li, S. Oda, T. Tanimura, T. Hoshida, and J. C. Rasmussen, "Low complexity digital perturbation back-propagation," presented at the 37th Eur. Conf. Expo. on Optical Communications, Geneva, Switzerland, 2011, Paper Tu.3.A.2.
[62] L. Li, Z. Tao, L. Dou, W. Yan, S. Oda, T. Tanimura, T. Hoshida, and J. C. Rasmussen, "Implementation efficient nonlinear equalizer based on correlated digital backpropagation," presented at the Optical Fiber Communication Conf., Los Angeles, CA, USA, 2011, Paper OWW3.
[63] T. Tanimura, S. Oda, T. Hoshida, L. Li, Z. Tao, and J. C. Rasmussen, "Experimental characterization of nonlinearity mitigation by digital back propagation and nonlinear polarization crosstalk canceller under high PMD condition," presented at the Optical Fiber Communication Conf., Los Angeles, CA, USA, 2011, Paper JWA020.
[64] Z. Tao, L. Dou, W. Yan, L. Li, T. Hoshida, and J. C. Rasmussen, "Multiplier-free intrachannel nonlinearity compensating algorithm operating at symbol rate," *J. Lightw. Technol.*, vol. 29, no. 17, pp. 2570–2576, Sep. 2011.
[65] G. Gao, X. Chen, and W. Shieh, "Influence of PMD on fiber nonlinearity compensation using digital back propagation," *Opt. Exp.*, vol. 20, pp. 14406–14418, 2012.
[66] H. Nakashima, T. Oyama, Y. Akiyama, S. Oda, L. Dou, Y. Fan, Z. Tao, T. Hoshida, and J. C. Rasmussen, "PMD and PDL tolerances of transmitter-side non-linear mitigation in 112 Gb/s DP-QPSK transmission," presented at the Eur. Conf. and Expo. on Optical Communications, Geneva, Switzerland, 2012, Paper We.3.C.5.
[67] K. Toyoda, Y. Koizumi, T. Omiya, M. Yoshida, T. Hirooka, and M. Nakazawa, "Marked performance improvement of 256 QAM transmission using a digital back-propagation method," *Opt. Exp.*, vol. 20, pp. 19815–19821, 2012.
[68] L. Dou, Z. Tao, Y. Akiyama, S. Oda, Y. Fan, T. Oyama, H. Nakashima, T. Hoshida, and J. C. Rasmussen, "Real-time 112Gb/s DWDM coherent transmission with 40% extended reach by transmitter-side low-complexity nonlinear mitigation," presented at the Eur. Conf. and Expo. on Optical Communications, Geneva, Switzerland, 2012, Paper Th.1.D.3.
[69] G. Shulkind and M. Nazarathy, "Nonlinear digital back propagation compensator for coherent optical OFDM based on factorizing the volterra series transfer function," *Opt. Exp.*, vol. 21, pp. 13145–13161, 2013.
[70] Y. Bao, Z. Li, J. Li, X. Feng, B. Guan, and G. Li, "Nonlinearity mitigation for high-speed optical OFDM transmitters using digital pre-distortion," *Opt. Exp.*, vol. 21, pp. 7354–7361, 2013.
[71] E. G. Turitsyna and S. K. Turitsyn, "Digital signal processing based on inverse scattering transform," *Opt. Lett.*, vol. 38, pp. 4186–4188, 2013.
[72] Y. Gao, J. C. Cartledge, A. S. Karar, S. S.-H. Yam, M. O'Sullivan, C. Laperle, A. Borowiec, and K. Roberts, "Reducing the complexity of perturbation based nonlinearity pre-compensation using symmetric EDC and pulse shaping," *Opt. Exp.*, vol. 22, pp. 1209–1219, 2014.
[73] Y. Gao, A. S. Karar, J. C. Cartledge, S. Yam, M. O'Sullivan, C. Laperle, A. Borowiec, and K. Roberts, "Simplified nonlinearity pre-compensation using a modified summation criteria and non-uniform power profile," presented at the Optical Fiber Communication Conf., San Francisco, CA, USA, 2014, Paper Tu3A.6.
[74] N. Alic and S. Radic, "Optical frequency combs for telecom and datacom applications," presented at the Optical Fiber Communication Conf., San Francisco, CA, USA, 2014, Paper W4E.4.
[75] B. P.-P. Kuo, E. Myslivets, V. Ataie, E. G. Temprana, N. Alic, and S. Radic, "Wideband parametric frequency comb as coherent optical carrier," *J. Lightw. Technol.*, vol. 31, no. 21, pp. 3414–3419, Nov. 2013.
[76] E. Myslivets, B. P. P. Kuo, N. Alic, and S. Radic, "Generation of wideband frequency combs by continuous-wave seeding of multistage mixers with synthesized dispersion," *Opt. Exp.*, vol. 20, pp. 3331–3344, 2012.
[77] V. Ataie, E. Myslivets, B. P.-P. Kuo, N. Alic, and S. Radic, "Spectrally equalized frequency comb generation in multistage parametric mixer with nonlinear pulse shaping," *J. Lightw. Technol.*, vol. 32, no. 4, pp. 840–846, Feb. 2014.
[78] B. P.-P. Kuo, E. Myslivets, N. Alic, and S. Radic, "Wavelength multicasting via frequency comb generation in a bandwidth-enhanced fiber optical parametric mixer," *J. Lightw. Technol.*, vol. 29, no. 23, pp. 3515–3522, Dec. 2011.
[79] Z. Tong, A. O. J. Wiberg, E. Myslivets, B. P. P. Kuo, N. Alic, and S. Radic, "Spectral linewidth preservation in parametric frequency combs seeded by dual pumps," *Opt. Exp.*, vol. 20, pp. 17610–17619, 2012.
[80] E. Temprana, V. Ataie, B. P.-P. Kuo, E. Myslivets, N. Alic, and S. Radic, "Low-noise parametric frequency comb for continuous C-plus-L-band 16-QAM channels generation," *Opt. Exp.*, vol. 22, pp. 6822–6828, 2014.
[81] V. Ataie, E. Temprana, L. Liu, Y. Myslivets, P. P. Kuo, N. Alic, and S. Radic, "Flex-grid compatible ultra wide frequency comb source for 31.8 Tb/s coherent transmission of 1520 UDWDM channels," presented at the Optical Fiber Communication Conf., San Francisco, CA, USA, 2014, Paper Th5B.7.
[82] G. P. Agrawal, *Nonlinear Fiber Optics*, 2nd ed. San Diego, CA, USA: Academic Press, 1995.
[83] M. Saha and A. K. Sarma, "Solitary wave solutions and modulation instability analysis of the nonlinear Schrodinger equation with higher order dispersion and nonlinear terms," *Commun. Nonlinear Sci. Numer. Simulat.*, vol. 18, pp. 2420–2425, 2013.
[84] J. Yang and K. R. Akylas, "Continuous families of embedded solitons in the third order nonlinear schrodinger equation," *Stud. Appl. Math.*, vol. 111, pp. 359–375, 2003.
[85] J. E. Prilepsky, S. A. Derevyanko, and S. K. Turitsyn, "Nonlinear spectral management: Linearization of the lossless fiber channel," *Opt. Exp.*, vol. 21, pp. 24344–24367, 2013.
[86] C. J. McKinstrie and N. Alic, "Information efficiencies of parametric devices," *IEEE J. Sel. Topics Quantum Electron.*, vol. 18, no. 2, pp. 794–811, Mar./Apr. 2012.
[87] S. Zhang, E. Mateo, L. Xu, M. Huang, F. Yaman, Y. Shao, T. Wang, Y. Inada, T. Inoue, T. Ogata, and Y. Aoki, "100 G upgrade over legacy submarine dispersion-managed fiber link using fiber nonlinearity compensation and maximum likelihood sequence estimation," presented at the Optical Fiber Communication Conf., Los Angeles, CA, USA, 2012, Paper OTu2A.4.
[88] Y. Huang, E. Mateo, M. Sato, D. Qian, F. Yaman, T. Inoue, Y. Inada, S. Zhang, Y. Aono, T. Tajima, T. Ogata, and Y. Aoki, "Real-time transoceanic transmission of 1-Tb/s nyquist superchannel at 2.86-b/s/Hz spectral efficiency," presented at the Asia Communications and Photonics Conf., Guangzhou, China, 2012, Paper PAF4C.2.
[89] T. Inoue, E. Mateo, F. Yaman, T. Wang, Y. Inada, T. Ogata, and Y. Aoki, "Low complexity nonlinearity compensation for 100 G DP-QPSK transmission over legacy NZ-DSF link with OOK channels," presented at the Eur. Conf. and Expo. on Optical Communications, Amsterdam, Netherlands, 2012, Paper Mo.1.C.5.
[90] A. Hasegawa and T. Nyu, "Eigenvalue communication," *J. Lightw. Technol.*, vol. 11, no. 3, pp. 395–399, Mar. 1993.
[91] R. Courant and D. Hilbert, *Methods of Mathematical Physics*. New York, NY, USA: Willey, 1989.
[92] J. G. Proakis and M. Salehi, *Digital Communications*, 5th ed. New York, NY, USA: McGraw-Hill, 2007.
[93] J. P. Gordon and L. F. Mollenauer, "Phase noise in photonic communications systems using linear amplifiers," *Opt. Lett.*, vol. 15, no. 23, pp. 1351–1353, 1990.
[94] (2014). [Online]. Available: http://www.emcore.com/wp-content/uploads/EMCORE-ITLA-High-Data-Rate-Application-Note.pdf
[95] (2014). [Online]. Available: http://cp.literature.agilent.com/litweb/pdf/5990–5512EN.pdf
[96] C. E. Shannon, "A mathematical theory of communication," *Bell Syst. Tech. J.*, vol. 27, pp. 379–423, 1948.
[97] M. Hirano, T. Haruna, Y. Tamura, T. Kawano, S. Ohnuki, Y. Yamamoto, Y. Koyano, and T. Sasaki, "Record low loss, record high FOM optical fiber with manufacturable process," presented at the Optical Fiber Communication Conf., Anaheim, CA, USA, 2013, Paper PDP.A5.7.

Authors' biographies not available at the time of publication.